

# **Features of Magnetic Field Fluctuations in the Ionosphere at Swarm Altitude**

P. De Michelis<sup>1</sup>, G. Consolini<sup>2</sup>, R. Tozzi<sup>1</sup>, F. Giannattasio<sup>1</sup>, V. Quattrocioni<sup>2</sup> and I. Coco<sup>1</sup>

<sup>1</sup>Istituto Nazionale di Geofisica e Vulcanologia, Rome, Italy

<sup>2</sup>INAF-Istituto di Astrofisica e Planetologia Spaziali, Rome, Italy

## **Abstract**

The magnetosphere-ionosphere system is recognized as a complex and active element affected by space weather and as a region where important scientific questions related to space weather impacts need to be answered. In this framework, there is a high priority on the understanding of how local, regional, and global-scale phenomena couple to produce observed responses across various scales. Turbulence provides one pathway by which energy cascades across scales from large to small ones where energy can be dissipated in the form of heating. The Swarm mission, that is a true multi-point and multi-purpose constellation, represents a unique opportunity to address some of these scientific questions. In detail, it gives us a chance of investigating the nature and the scaling features of magnetic field fluctuations for different geomagnetic activity levels, and unveiling the role played by turbulence of ionospheric plasma medium on the magnetic field fluctuations. Recently, using Swarm magnetic field data at high-latitude in the Northern Hemisphere, the local scaling indices of the 1st and 2nd order structure functions of the magnetic field fluctuations have been evaluated, showing their capability both to give new insights about the ionosphere-magnetosphere coupling and to provide information on the ionospheric turbulence. Here, we improve and extend the analysis by investigating the scaling features of the geomagnetic field fluctuations of external origin, recorded by Swarm A satellite during a period of 2 years (April 2014–March 2016). Maps of the local Hurst exponent values, which allow us to study scaling properties of the geomagnetic field's spatial fluctuations are shown, both at high-latitudes (in the Northern and Southern Hemisphere) and at low- and mid-latitudes ( $\pm 60^\circ$ ) according to two different geomagnetic activity conditions. The aim is to capture the essential features of the spatial fluctuations of the geomagnetic field and understand their origins.

## **1. Introduction**

There is a growing body of literature that recognises the importance of the turbulence and intermittent phenomena in the ionospheric environment. Fluctuations of plasma density, electrostatic potential and magnetic and electric fields have confirmed the existence of a turbulent state in the ionosphere. This state, which can be detected at different spatial scales, is mainly the result of the various phenomena characterising the different magnetospheric regions coupled to the ionosphere via the geomagnetic field lines.

It has been shown that the turbulent character of the ionospheric plasma density plays an important role in the formation and dynamics of ionospheric inhomogeneities, which can have a great impact, for example, on the propagation of electromagnetic waves. These inhomogeneities, indeed, may affect the Global Navigation Satellite System (GNSS) performance, being responsible for different problems: from a simple signal delay to its total loss in case of scintillation events up to the production of misleading information due to strong ionospheric gradients. That is the reason why it has been recognized that plasma density plays a key role in the ionospheric processes.

Actually, other physical quantities, often underestimated, can play a crucial role in this framework and provide interesting information on the features of turbulence in the ionospheric environment. Since the work of Kintner and Seyler (1985), the turbulent properties of electric and magnetic fluctuations observed by rockets and spacecraft at different altitudes have been addressed in several papers. Great attention was especially paid to the analysis of turbulent properties of the high-latitude electric fluctuations trying to understand the nature of the phenomenon and to clarify its driving mechanisms. Many interesting features of electric field fluctuations were obtained using both data from low-altitude polar-orbiting Dynamic Explorer 2 (DE2) spacecraft during its several crossings of the auroral zone and polar cap under different interplanetary magnetic field orientations (Golovchanskaya et al., 2006; Golovchanskaya and Kozelov, 2010) and data based on ground-based stations and rockets measurements. These works suggested that small-scale electric and magnetic fields in the auroral zone are due to intermittent ionospheric turbulence, which develops in the regions of large-scale field-aligned currents (see, e.g., Kintner, 1976; Weimer et al., 1985; Basu et al., 1988; Tam et al., 2005; Golovchanskaya et al., 2006; Kozelov and Golovchanskaya, 2006; Kozelov et al., 2008). Some theories associated the observed ionospheric turbulence with structures of magnetospheric origin (e.g., Golovchanskaya et al., 2006) driven, for example, by shear flow instabilities. Other studies related the ionospheric turbulence directly to turbulence in the solar wind (e.g., Parkinson, 2006; Abel et al., 2009). Ionospheric turbulence in the form of spatial and temporal fluctuations of

plasma density has often been observed also at mid and low latitudes (Le et al., 2003; Molchanov et al., 2004). The irregularities, resulting from a variety of plasma instabilities associated with perturbations in the complex arrangement of electric and magnetic field, were observed by ground-based coherent and incoherent scatter radars, sounding rockets and satellites. For example, Jahn and LaBelle (1998) presented one of the first rocket measurements of equatorial spread F irregularities at altitudes above 600 km, showing how power spectra of the electron density fluctuations were characterised by dual-power law behaviour. Based on plasma density data from the Cosmos-900 satellite Molchanov et al. (2004) analysed the spatial distribution of the ionospheric turbulence (in the spatial range between 15 and 300 km) at the satellite height  $h=450\text{--}500$  km and found a power density spectrum in the case of both the plasma and the electric field in the analysed regions. Bhattacharyya (1990) studied the chaotic behaviour of ionospheric density fluctuations, using amplitude and phase scintillation data, and found the existence of low-dimensional chaos. The same chaotic behaviour of ionospheric turbulence was also investigated by Wernik and Yeh (1994) using scintillation data and numerical modelling of scintillation at high-latitude. A unified picture of plasma irregularities in equatorial spread F was developed from the analysis of satellite, sounding rocket, and coherent scatter radar observations by Hysell (2000) in his interesting overview of equatorial ionospheric turbulent conditions.

It is important to notice that the spatial features of plasma density irregularities have a wide range of scale sizes, spanning from centimeters to hundreds or perhaps thousands of kilometers. This observed broad range of irregularity scale sizes, which is indicative of nonlinear mode-coupling, exhibits a power-law scaling, with variable spectral indices. During recent years, large variations of the spectral index, used to describe the ionospheric turbulence, were registered to be dependent on the different geomagnetic conditions of observations.

The European Space Agency minisatellite constellation mission, called Swarm, can be extremely useful in this context. Indeed, thanks to both the inclination of the orbits and the precession of their planes, Swarm satellites ensure a global coverage in a few months (Friis-Christensen et al., 2006). Data recorded by these satellites can be consequently used to statistically analyse the features of magnetic field fluctuations across the globe.

In this framework, we characterise the features of magnetic field fluctuations in the F-region of the ionosphere using measurements recorded by the Swarm A satellite during a period of two years (April 2014 – March 2016). The fluctuations are described under the assumption that, according to previous findings, they obey a power-law distribution. Under this assumption, we consider the horizontal magnetic field intensity of magnetospheric and ionospheric origin and analyse the changes in the scaling properties of its spatial/temporal fluctuations, which are valid

for a certain range of scales. To do this, we evaluate the local Hurst exponent, that characterises the time fluctuations observed in a signal defining their degree of persistence or anti-persistence, and discuss the changes in the Hurst exponent values in relation to the most important ionospheric and magnetospheric current systems, which could reveal the nature of the magnetic field fluctuations.

The paper is organised as follows. At first, the data sources are discussed, and then, a brief summary of the method of analysis is presented. Following this, the analysis is applied on the selected data in three different latitudinal regions: Northern high latitudes, middle and low latitudes and Southern high latitudes. Finally, the implications of findings are discussed.

## 2. Data

This study is based on in situ observations of the geomagnetic field recorded on Swarm A, one of the three satellites of Swarm constellation, in the F-region of the ionosphere. The minisatellite Swarm constellation consists of three identical satellites, which fly in two different orbital planes at two different altitudes. Two satellites (Swarm A and Swarm C) fly side-by-side at a mean altitude of approximately 460 km in a plane of 87.4° inclination, while the third satellite (Swarm B) orbits 50 km above in a plane of 88° inclination (Friis-Christensen et al., 2006). In this study we consider low-resolution (1 Hz) geomagnetic field observations from Swarm A in the time interval from 1 April 2014 to 31 March 2016. We use SW\_OPER\_MAGA\_LR\_1B data file types, with file counter equal to 0408 according to ESA nomenclature. They are available at <ftp://swarm-diss.eo.esa.int> upon registration. Such data provided us with the UTC time, the altitude of the satellite (in km), the satellite position (in local geographic latitude and longitude) and the vector magnetic field in the North-East-Center (NEC) frame of reference (in nT).

We use the CHAOS-6 geomagnetic field model (Finlay et al., 2016) to remove from the observed magnetic data the main field and its secular variation. CHAOS-6 is a high-resolution geomagnetic model, which spans a period between 1997 and 2016, and it is obtained from satellite magnetic data (Swarm, CHAMP, and Ørsted) along with ground observatory data (Finlay et al., 2015). Thus, from the original data we remove the contribution coming from the internal field modelled by CHAOS-6 to obtain the external magnetic field of magnetospheric and ionospheric origin along the three magnetic field components. From the  $B_X$  (Northward) and  $B_Y$  (Eastward) components of the geomagnetic field of external origin in the NEC (North-East-Centre) frame of reference we evaluate the intensity of the horizontal magnetic field component  $B_H = (B_X^2 + B_Y^2)^{1/2}$ , which is analysed in three different latitudinal regions: Northern high latitudes (magnetic latitude  $> 50^\circ$  N), mid- and low-latitudes (within  $\pm 60^\circ$  magnetic latitude) and Southern high latitudes ( $> 50^\circ$  S) and according to two different geomagnetic

activity levels. The Auroral Electrojet index (AE) and SYM-H index are used to discriminate between quiet and active periods. The AE index is used to monitor the level of geomagnetic disturbance resulting from the auroral electrojets, being a proxy of the total currents in the auroral zone, while the SYM-H index gives information about the strength of the ring current around the Earth, which increases during disturbed periods. To select geomagnetically quiet periods we consider the following simultaneous conditions:  $AE < 60$  nT and  $-5$  nT  $< SYM-H < 5$  nT. In this way the chosen time periods are supposed to be devoid of the magnetic perturbations introduced by the occurrence of storm and substorm events. On the other hand, to select active periods we consider the following simultaneous conditions:  $AE > 100$  nT and  $SYM-H < -30$  nT. In this case, the chosen time periods can be reasonably considered to capture the external perturbations induced by magnetic storm events. The geomagnetic storms are primarily responsible for geomagnetic variations at low and mid-latitudes, while the geomagnetic substorms, which usually influence the geomagnetic field at high latitudes, can also contaminate the magnetic observations at lower latitudes due to the equatorward expansion of the auroral ovals during intense events. These choices of geomagnetic activity levels, which differ from previous works (e.g. De Michelis et al, 2015), are chosen to ensure a manageable data set since the simultaneous use of constrains on AE and SYM-H strongly reduces the amount of available data for each level. The AE and SYM-H data with one minute cadence can be downloaded from the OMNI website ([www.cdaweb.gsfc.nasa.gov/istp-public/](http://www.cdaweb.gsfc.nasa.gov/istp-public/)).

Data are presented in terms of a quasi-dipole (QD) coordinate system, which is an apex system, introduced by Richmond (1995), and organized with respect to the Sun position introducing the magnetic local time (MLT), which is evaluated using the common definition given by Baker and Wing (1989). It has been shown, indeed, that this coordinate representation of the data in the QD coordinate system is most appropriate when analysing data in terms of ionospheric currents, which are fixed with respect to the Sun (Laundal and Gjerloev, 2014).

### 3. Method of analysis

To investigate the magnetic spatial fluctuation features we adopt the same method used in our previous studies (De Michelis et al., 2015, 2016, 2017) that is based on structure function analysis, a methodology that is widely used in different fields where turbulence phenomena and scale-invariant features play a fundamental role (Frisch, 1995). In detail, we evaluate the first-order structure function  $S_1$  defined according to the following equation:

$$S_1(\tau) = \langle |B_H(t + \tau) - B_H(t)|^{\gamma(1)} \rangle_T \quad (1)$$

where  $B_H(t)$  is the time series to be analysed,  $\langle \rangle$  denotes an ensemble average of the increments of the variable taken over all pairs of points separated by a scale  $\tau$  that quantifies the scale of interest, and  $T$  is the time interval over which the average is calculated. In the case of a scale-invariant signal, the first-order structure function,  $S_1(\tau)$ , depends on the scale  $\tau$  by a power-law,  $S_1(\tau) \sim \tau^{\gamma(1)}$ , where the scaling exponent,  $\gamma(1)$ , permits us to characterise the spatiotemporal structure of the analysed signal by describing the rescaling of the signal variance at different scales of observation. In first approximation, it can be considered equivalent to the Hurst exponent ( $H$ ), which is commonly utilized to describe stochastic processes (Hurst, 1956). The Hurst exponent, whose values range in the interval  $[0, 1]$ , permits us to analyse the features of the magnetic field fluctuations, indicating the presence of fluctuations, that tend to cluster along a direction as a consequence of their persistent character ( $H > 0.5$ ) or fluctuations that tend to induce stability in the system due to their anti-persistent character ( $H < 0.5$ ) and regress strongly to the mean. Different methods are available to extract the scaling exponents of the structure functions. For example, wavelet based methodologies, Hilbert-based method, or the scaling analysis of probability density function of increments, to name a few. Each method has its own advantages and shortcomings. In this paper, a detrended structure-function (DSF) method is proposed to extract scaling exponents (De Michelis et al., 2015, 2016, 2017). This is accomplished by removing a polynomial trend within a window size  $T$  before calculating the increment. This procedure is designated as detrending analysis. By doing so, scales larger than  $T$  are expected to be removed or constrained and the method acts as a high-pass filter in temporal domain.

In detail, we consider a moving window of  $T=400$  s, and in each time window we construct a detrended time series,  $B_{H,d}(t)$ , obtained from subtracting to the original time series, which is in our case the intensity of the horizontal component of the geomagnetic field of external origin, its average long-term trend. The latter is obtained using a polynomial fit so to eliminate all possible spurious effects. On each time window, the detrended time series  $B_{H,d}(t)$  is used to evaluate the first-order structure function considering as scales of interest those in the interval  $\tau \in [1 - 40]$  s. The maximum scale investigated (40 s) is 10 times smaller than the size of moving window (400 s) used; this ensures the reliable estimation of the 40 s fluctuation statistics.

Figure 1 reports an example of the behaviour of the first-order structure function  $S_1(\tau)$ . A clear power law dependence is recovered at the scales investigated here, thus assessing the scale invariance of the analysed signal in the considered range of timescales.

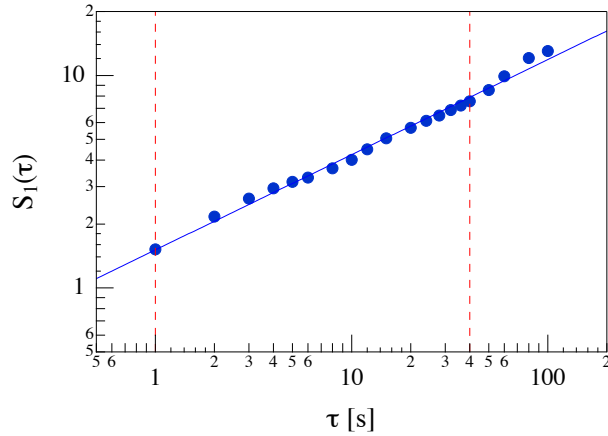


**Figure 1.** An example of the behaviour of the first-order structure function  $S_1(\tau)$  during an high-latitude crossing in the Northern Hemisphere. Power-law behaviour is observed in the range analysed (between the two vertical dashed lines) with a scaling exponent  $H = (0.45 \pm 0.01)$ .

Under the Taylor’s hypothesis or the “frozen turbulence approximation” (Taylor, 1938) we can relate the temporal scale to the spatial one. A condition for the validity of this assumption is that the temporal variations of the spatial structures occur on time scales longer than the transit time of the satellite in these structures. This assumption was checked in our previous work (De Michelis et al., 2017) using magnetic measurements recorded simultaneously by Swarm A and C, the two satellites of the Swarm constellation which orbit side by side at a distance of about 160 km near the equator and transit in the same region with a time delay of about 10 s. Thus, under this assumption and in first approximation, the analysis of the time scales of the geomagnetic field fluctuations in the interval [1–40] s corresponds to the analysis of spatial scales in the interval between 8 km and ~300 km, being the velocity of the Swarm satellites about 7.6 km/s.

#### 4. Results and discussions

Figure 2 reports the local Hurst exponent values during both quiet (top panel) and active (bottom panel) geomagnetic conditions obtained by analysing the fluctuations of the horizontal intensity of the external geomagnetic field at low and middle magnetic latitudes ( $\pm 60^\circ$ ). Figure 2 allows us to distinguish regions where the geomagnetic field fluctuations have a persistent character (in blue) from those characterised by an anti-persistent one (in red). At low and mid-latitude ( $\pm 40^\circ$ ), before and after noon (from 06:00 MLT to 18:00 MLT), the geomagnetic field fluctuations have always a strong persistent character ( $H > 0.7$ ) independently from the geomagnetic activity levels. In the other regions, the geomagnetic field fluctuations generally exhibit a small persistent character ( $H \sim 0.6$ ). Variations from a quasi anti-persistent character to

a persistent one appear at higher latitudes ( $> |50|^\circ$ ) before and after midnight (from 18:00 MLT to 06:00 MLT) during geomagnetically active periods. Furthermore, during active periods we observe an increase of the persistent character also at mid- and low-latitudes in the dusk-to-dawn sector (from 18:00 MLT to 06:00 MLT).

These latitudinal structures observed in the spatial patterns of the Hurst exponent are expected to result from different physical processes in terms of currents and convection processes, which can cause the different features of the magnetic field fluctuations. In detail, the possible sources of the fluctuations observed on the external component of the geomagnetic field here considered have to be searched among the time-varying electric currents flowing in the ionosphere responsible for signals whose superposition produce the recorded Earth's magnetic field of external origin. At low and mid latitudes these latitudinal structures are responsible for macroscopic variations observed also during geomagnetically quiet conditions, namely for both the regular daily variation of the geomagnetic field, which is referred to as solar quiet variation, and the so-called equatorial electrojet current.

The equatorial electrojet (EEJ) is an intense eastward electric current flowing on the day-side, in a narrow band of a few hundred kilometers along the dip equator in the ionospheric E-region (90 to 150 km altitude range). It is most intense over a time period that extends from 10:00 to 14:00 LT and reaches its maximum intensity between 11:00 and 12:00 LT (Onwumechili, 1997). Outside of this LT sector, the EEJ decreases significantly and usually diminishes at night-time. This strong horizontal current causes a magnetic field disturbance, which weakens the horizontal component of the terrestrial magnetic field at the Earth's surface over a distance of about 600 km across the equator producing an effect similar to that due to the ring current.

The solar quiet daily variation (Sq) mainly arises from the ionospheric current system flowing in the so-called dynamo region. This current system, that can be quite well approximated by a 2-D current flowing in the ionospheric E-region between 90 and 130 km (Chapman, 1929; Richmond et al., 1976), is driven by different processes. It is associated with expansion and contraction of the atmosphere as the Sun rises and sets daily, with the global scale horizontal upper-atmosphere winds, with the lunar tidal forces on the region, and with variations of Sun's electromagnetic emissions responsible for extra photoionization of the region. As a result, Sq variation is a function of latitude, local time, season and solar activity level (Campbell, 2003). The basic pattern of the equivalent Sq current system consists in a near-two-dimensional current circuit at  $\sim 110$  km altitude fixed with respect to the Earth-Sun line, and flowing in counter-clockwise direction in the Northern Hemisphere and clockwise direction in the Southern Hemisphere. The centres of the current vortices lie around  $40^\circ$  North or South magnetic latitude. The Sq variation is responsible of an enhancement in the value of the horizontal



component shortly before 06:00 LT with the rising of the sun, which reaches its maximum at about 11:00 LT and then comes back to the night time value at 16:00 LT, remaining constant throughout most of the night. Of course, the Sq variation of the horizontal component of the geomagnetic field, which occurs in both hemispheres, is superimposed onto the variation produced by the EEJ at low latitudes near the geomagnetic equator.

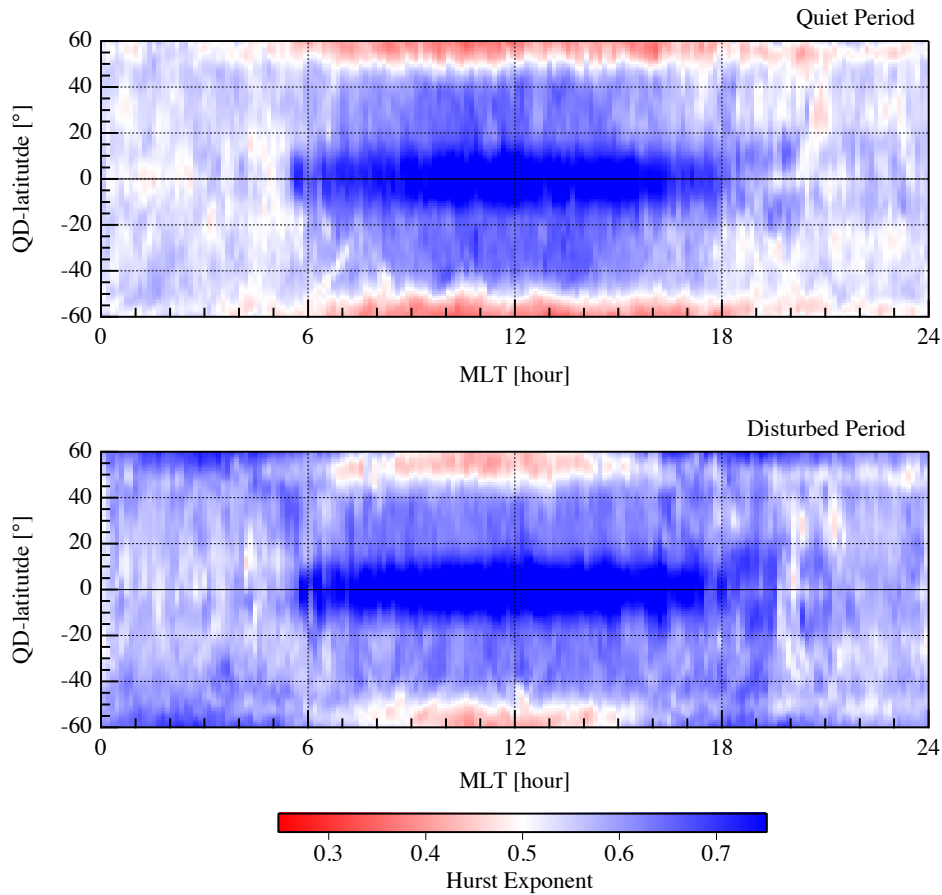


**Figure 2.** Local Hurst exponent values during both quiet (top panel) and active (bottom panel) geomagnetic conditions at low and middle QD magnetic latitudes ( $\pm 60^\circ$ ) as function of MLT.

Thus, the persistent character of the magnetic field fluctuations seems to correspond with those regions where the intensity of the horizontal component of the magnetic field changes as a consequence of different ionospheric current systems. These current systems develop over spatial scale larger than 300 km and consequently they may be responsible, at the lower spatial scales that we are examining (8-300 km), for the persistent character of the fluctuations that will tend to cluster in a direction.

When the geomagnetic activity level increases passing from a quiet period to an active one, the

spatial distribution of the  $H$  values remains essentially the same at low and mid latitudes around noon. There is an increase of the persistent character in the dusk-to-dawn sector, which can be associated with the increase of equatorial currents flowing in the magnetosphere that intensify during active periods. The most important variations of the  $H$  values occur indeed in the higher latitude portion of the considered map, and in the nightside sector from the 18:00 to 06:00 MLT in both hemispheres. These variations could be related to the auroral electrojets, which are known to shift equatorward drastically during disturbed periods. Indeed, it has been found that during the main phase of intense storms, the westward electrojet can cover the latitudes from  $50^\circ$  to  $80^\circ$  on the nightside while the eastward electrojet, which flows in the dusk sector, can extend to latitudes even lower than those of the westward electrojet.

It is interesting to notice that during disturbed periods the global ionospheric electric field and currents increase in magnitude and exhibit rapid fluctuations. The disturbed magnetic perturbations are associated only partly with the ionospheric currents, since a substantial portion comes from more distant magnetospheric currents like the ring current, the magnetotail current and the field aligned currents. The increase of the persistent character of fluctuations observed both at high latitudes and in the dusk-to-dawn sector of the equatorial region during active periods is an effect of the increase of both the westward auroral electrojet and the ring current. This result agrees with the increase of the persistent character of AE and Dst fluctuations during disturbed times (see e.g. Uritsky and Pudovkin, 1998; Balasis et al., 2006). It is also important to notice that in the dip equatorial region the magnetic field is nearly parallel to the Earth's surface and the horizontal component describes completely the Earth's magnetic field. This provides a constraint on the motion of the charged particles that comprise the ionosphere and produces distinctive behaviour in the equatorial ionosphere. The so-called fountain effect of the ionospheric plasma creates a condition that enhances the growth of the Rayleigh-Taylor (RT) instability. The density depletion referred to as an equatorial plasma bubble (EPB) may rise to the topside of the equatorial F region and also develop smaller scale structure. In recent years, magnetic field fluctuations associated with EPBs have also been observed. They are significant only in the components transverse to the main geomagnetic field, which are directed along the z-axis in the equatorial region. This explains the persistent behaviour of the magnetic field fluctuations that are clustered in a direction inhibited by the strong magnetic field, especially around the dip equatorial region.

To better visualize the changes of the  $H$  values at high latitudes, in Figure 3 we show polar maps of the large-scale spatial distribution of the  $H$  values both in the Northern high latitudes ( $50^\circ$  N –  $90^\circ$  N) and in the Southern high latitudes ( $50^\circ$  S –  $90^\circ$  S). In detail, the  $H$  values in the Northern

Hemisphere are shown on the left for quiet (upper left panel) and active (lower left panel) periods, while the  $H$  values relative to the Southern high latitudes are shown on the right panels of the same figure for the two different activity conditions: quiet (upper right panel) and active (lower right panel).

The features of the magnetic field fluctuations are similar in the two hemispheres during both quiet and active conditions. During quiet geomagnetic conditions, the  $H$  values show a strong asymmetry in the daily character of the magnetic field fluctuations. They exhibit an anti-persistent character in the sunlit hemisphere ( $05:00 < \text{MLT} < 18:00$ ) and a mostly persistent one in the dark sector in a band of magnetic latitude between  $\sim 50^\circ$  and  $75^\circ$  in both hemispheres. These maps are slightly different from previous results reported by De Michelis et al. (2015) where the fluctuations of the horizontal component of the Earth's magnetic field from 1 January 2014 to 30 June 2014 were analysed and the Hurst exponent evaluated. The difference in the obtained results, which are localized essentially in the polar cap regions, can be due to different datasets utilized in the two works. Here, we have removed from the original data (2 years instead of 6 months) the contribution coming from the internal field produced by the CHAOS-6 model to obtain a dataset that describes only the magnetic field which is caused by magnetospheric and ionospheric currents and used different conditions for defining the quiet and disturbed geomagnetic activity levels.

During active periods, the region with an anti-persistent character becomes smaller. It is localized mainly in a narrow band between  $50^\circ$  and  $60^\circ$  in the sunlight sector. Conversely, the persistent region shows an increasing equatorward extent in the dark sector. The only anomaly, with respect to our previous results (De Michelis et al. 2015), is represented by the polar cap region, where the  $H$  values are always less than 0.5 describing a constant anti-persistent character of the geomagnetic field fluctuations regardless of the geomagnetic activity level.

Also in this case, the observed difference in the character of magnetic field fluctuations reflects the morphology and dynamics of that part of the ionosphere, which is crossed by the satellite. At high-latitude the ionosphere differs significantly from its mid-latitude counterpart. The high-latitude ionosphere is characterised by a strong coupling between the magnetosphere and ionosphere through electric fields and currents as well as particle flows, which make the description of this ionospheric region difficult. It is known that this region is more directly modified by magnetospheric processes that are largely controlled by the interaction between the solar wind and the Earth's magnetosphere. Indeed, at these latitudes the ionospheric currents are joined with currents flowing along geomagnetic field lines into the magnetosphere and their electrodynamic is dominated by the influences of magnetospheric processes.

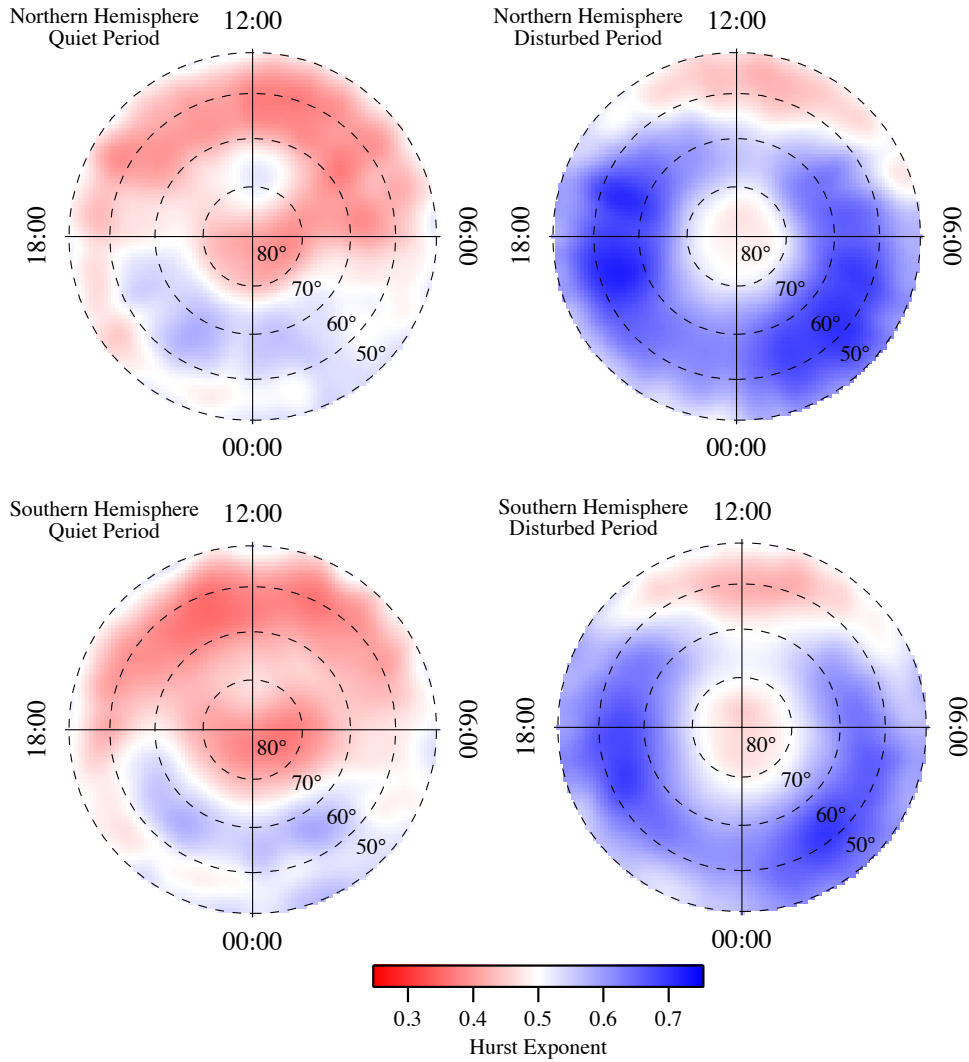


**Figure 3.** The local Hurst exponent values in the Northern high latitudes (top) and Southern high latitudes (bottom) in a polar representation of magnetic local time (MLT) and magnetic latitude. The maps refer to (left) quiet ( $AE < 60$  nT and  $-5$  nT  $< SYM-H < 5$  nT) and (right) disturbed ( $AE > 100$  nT and  $SYM-H < -30$  nT) conditions. Dashed circles are drawn at  $QD$  magnetic latitudes of  $50^\circ$ ,  $60^\circ$ ,  $70^\circ$ , and  $80^\circ$ .

At high-latitude and low altitude there are two major constituents of magnetic field fluctuations: (1) electric currents in the ionospheric E-layer (at an altitude of about 110 km) flowing on a horizontal plane that practically perpendicular to the ambient magnetic field and can be decomposed into Hall and Pedersen currents; and (2) currents flowing along the magnetic field lines connecting the ionosphere and the magnetosphere (FACs). In both cases, due to the significant ionisation caused by particles precipitating into the auroral oval, the high-latitude

current flow is concentrated inside the auroral oval, where it forms the auroral electrojets, which are the most prominent currents at auroral latitudes. They consist of eastward and westward components that are primarily Hall currents originated around noon, and are fed by downward FACs connecting the ionosphere in the nightside to the magnetospheric current wedge. During disturbed periods, the ionospheric current flow is strongly enhanced, there is the formation of a substorm electrojet with strongly enhanced westward current flow in the midnight sector and all the current structure expands to lower latitudes. The distribution and the intensity of these currents depend indeed on the magnetic activity and the interplanetary magnetic field orientation. Thus, the regions characterised by a persistent behaviour of the magnetic field fluctuations seem to correspond closely with those characterised by intense ionospheric current systems and plasma convection processes.

One feature of a self-affine time series, which means of a time series whose rescaled version of a small part has the same statistical distribution as the larger part, is that its power-spectral density is defined as a power-law function of the frequency, whose exponent,  $\beta$ , is directly linked to the Hurst exponent through the following relationship:  $\beta = 2H + 1$ . This means that the ionospheric regions characterised by different  $H$  values have different behaviours of the spectral density. In our case the geomagnetic field's spectral density is therefore characterised by  $\beta > 2$  ( $\beta \sim 2.5-2.6$ ) in those regions where the Hurst exponent assumes values greater than 0.5 (for instance, in the auroral oval and at mid and low latitudes in the dayside), while the spectral exponent is  $\beta < 2$  ( $\beta \sim 1.6-1.8$ ) in those regions with  $H$  values smaller than 0.5 (in the polar cap, in the dayside sector at high latitude during quiet periods and in the nightside sector at mid and low latitudes regardless of geomagnetic activity level).

Similar values of spectral indices have been found analysing the ionospheric electric field fluctuation spectra. Values of spectral index greater than 2.5 have been associated with regions characterised by stronger shear flows and enhanced field intensity (Kinter and Seyler, 1985). We can extend this interpretation also to the case of magnetic field fluctuations. However, it is difficult to identify the shear in the flow as the primary driving mechanism of the observed spectra, as other mechanisms such as drift waves or a current-convective process could be responsible of them. For example, Ossakow and Chaturvedi (1979) and Chaturvedi and Ossakow (1981) discussed the current-convective instability in the context of irregularities in the auroral ionosphere, suggesting the important role played by this process in the ionospheric regions. This hypothesis was confirmed by Basu et al. (1984), who found that in the spatial region of strong shear flow, the density fluctuation spectrum was relatively flat, while outside the shear flow regions, but staying within the electron precipitation region, the density fluctuation spectrum steepened to an index between - 2.0 and - 3.0 which was consistent with a current-

convective process. These previous results seem to confirm our hypothesis according to which the regions characterised by a persistent behaviour of the magnetic field fluctuations correspond closely with those characterized by intense ionospheric current systems and plasma convection processes. Consequently, mechanisms such as the shear flow or the current-convective process may be the main responsible of the magnetic field fluctuations features.

## 5. Summary and Conclusions

Data series generated by complex systems exhibits fluctuations on a wide range of time scales and/or broad distributions of the values. The natural fluctuations are often found to follow a scaling relation over several orders of magnitude. When this happens the dynamics of the system, described by the analysed time series, is usually denoted as fractal or multifractal, depending on the question if it is characterised by one scaling exponent or by a multitude of scaling exponents. It has been shown that the self-similar (scaling) and fractal properties may characterise, for example, the structure of Pedersen and Hall conductivities in the auroral zone and the magnetic and electric field fluctuations at small-scale.

The aim of this work was to extend the analysis of the scaling features of magnetic field fluctuations, which had been mainly confined to auroral regions in the previous work, to the whole globe. For this reason, the time series of the horizontal intensity of the external geomagnetic field, measured by Swarm A satellite over 2 years (from 1 April 2014 to 31 March 2016), were statistically analysed in terms of their scaling features. The first-order structure function scaling exponent (Hurst exponent) of the horizontal intensity was evaluated during quiet and disturbed geomagnetic activity periods at different latitudes. This study was performed in the temporal domain using the continuous 1s measurements taken by Swarm A along its orbit. From these time series, the spatial structures were inferred under Taylor's hypothesis. The values of the Hurst exponent were analysed according to three different latitudinal regions (Northern high latitudes, mid and low latitudes, Southern high latitudes) and two geomagnetic activity conditions (quiet and disturbed). What is interesting about the Hurst exponent values reported in Figures 2 and 3 is that they seem to localise different latitudinal structures. There are regions characterised by a persistent behaviour of the magnetic field fluctuations and regions where the fluctuations of the geomagnetic field exhibit an anti-persistent character. The regions characterised by magnetic field fluctuations with a larger value of the  $H$  exponent, which describe magnetic field fluctuations with a larger spatio/temporal coherence than the regions with a smaller  $H$  values, seem to correspond closely with regions characterized by ionospheric current system and plasma convection processes.

In our previous paper (De Michelis et al., 2017), by analysing the high-latitude geomagnetic

field fluctuations in the Northern Hemisphere, we found that these fluctuations were characterised by a high coherence inside convective ionospheric structures and by a lower degree of coherence along the boundaries of the convective structures. These results suggested that plasma dynamics play an important role in the coherence range of geomagnetic fluctuations. The conclusions derived from the Northern high latitude analysis seem to be supported by the analysis reported in this work, where the Southern high latitudes and the mid and low latitude regions have also been considered. Ionospheric and magnetospheric current systems and plasma convection processes in the equatorial region, at mid latitudes, and at high latitudes determine the scaling features (persistence or anti-persistence) of magnetic fluctuations at small spatial scales (8-300 km). The primary mechanisms that seem to control these scaling features are probably the shear motions in the plasma flow or the current-convective processes.

### **Acknowledgements**

The results presented in this paper rely on data collected by one of the three satellites of the Swarm constellation. We thank the European Space Agency (ESA) that supports the Swarm mission. Swarm data can be accessed online at <http://earth.esa.int/swarm>. The authors kindly acknowledge V. Papitashvili and J. King at the National Space Science Data Center of the Goddard Space Flight Center for the use permission of 1 min OMNI data and the NASA CDAWeb team for making these data available. Giuseppe Consolini and Virgilio Quattrocioni thank the Italian Space Agency (ASI) for the financial/funding support under project ASI “LIMADOU Scienza”.

### **References**

1. Abel, G.A., Freeman, M.P., Chisham, G., IMF clock angle control of multifractality in ionospheric velocity fluctuations. *Geophys. Res. Lett.* 36, 19102 (2009).
2. Baker, N.B. and Wing S., A new magnetic coordinate system for conjugate studies at high latitudes. *J. Geophys. Res.* 94, 9139 (1989).
3. Basu, S., Basu, S., MacKenzie, E., Fougere, P.F., Coley, W.R., Maynard, N.C., Winningham, J.D., Sugiura, M., Hanson, W.B., and Hoegy, W.R., Simultaneous Density and Electric Field Fluctuation Spectra Associated with Velocity Shears in the Auroral Oval, *J. Geophys. Res.*, 93A, 115 (1988).
4. Balasis G. et al., From pre-storm activity to magnetic storms: a transition described in terms of fractal dynamics, *Annales Geophysicae*, 24, 3557 (2006).

5. Bhattacharyya, A.: Chaotic behaviour of ionospheric turbulence from scintillation measurements, *J. Geophys. Res.*, 17, 733–738, (1990).
6. Campbell, W. H.: Introduction to geomagnetic fields, 2nd Edition, Cambridge University Press, (2003).
7. Chapman, S.: On the theory of the solar diurnal variation of the Earth's magnetism, *Proc. R. Soc. Lond. Ser. A*, 129, 369 (1929).
8. Chaturvedi, P. K. and Ossakow S. L., The Current Convective Instability as Applied to the Auroral Ionosphere, *J. Geophys. Res.* 86, 4411 (1981).
9. De Michelis, P., Consolini G., and Tozzi R., Magnetic field fluctuation features at Swarm's altitude: A fractal approach, *Geophys. Res. Lett.*, 42, 3100 -- 3105, doi:10.1002/2015GL063603 (2015).
10. De Michelis, P., Consolini G., Tozzi R., and Marcucci M. F., Observations of high-latitude geomagnetic field fluctuations during ST. Patrick's Day storm: Swarm and SuperDARN measurements, *Earth, Planets and Space*, 68, 105, doi: 10.1186/s40623-016-0476-3 (2016).
11. De Michelis, P., Consolini G., Tozzi R., and Marcucci M. F., Scaling features of high latitude geomagnetic field fluctuations at Swarm altitude: Impact of IMF orientation, *J. Geophys. Res. Space Phys.*, doi:10.1002/2017JA024156 (2017).
12. Finlay, C. C., DTU candidate field models for IGRF-12 and the CHAOS-5 geomagnetic field model, *Earth, Planets and Space* 67, 114 (2015).
13. Finlay, C.C., Lesur V., Thébault E., Vervelidou F., Morschhauser A., Shore R., Challenges handling magnetospheric and ionospheric signals in internal geomagnetic field modelling. *Space Sci. Rev.* doi: 10.1007/s11214-016-0285-9 (2016).
14. Friis-Christensen, E., Lühr H., and Hulot G., Swarm: a constellation to study the earth's magnetic field, *Earth Planets Space*, 58, 351 (2006).
15. Frisch, U., *Turbulence: The Legacy of A. N. Kolmogorov*, 89 pp., Cambridge Univ. Press, New York (1995).
16. Golovchanskaya, I. V., Ostapenko A. A., and Kozelov B. V., Relationship between the high-latitude electric and magnetic turbulence and the Birkeland field-aligned currents, *J. Geophys. Res.*, 111, A12301, doi:10.1029/2006JA011835 (2006).
17. Golovchanskaya, I. V., and Kozelov B. V., On the origin of electric turbulence in the polar cap ionosphere, *J. Geophys. Res.*, 115, A09321, doi:10.1029/2009JA014632 (2010).
18. Hysell, D. E., An overview and synthesis of plasma irregularities in equatorial spread F, *JASTP*, 62, 1037-1056 (2000).



19. Hurst, H., Methods of using long-term storage in reservoirs. *ICE Proceedings*, 5, 704, 519–543 (1956).
20. Kintner, P.M., Jr., Observations of Velocity Shear Driven Plasma Turbulence, *J. Geophys. Res.*, 81, 5114, (1976).
21. Kintner, P. M., and Seyler C. E., The status of observations and theory of high latitude ionospheric and magnetospheric plasma turbulence, *Space Science Reviews* 41 91-129 (1985).
22. Kozelov, B. V., and Golovchanskaya I. V., Scaling of electric field fluctuations associated with the aurora during northward IMF, *Geophys. Res. Lett.*, 33, L20109, doi:10.1029/2006GL027798 (2006).
23. Kozelov, B.V., Golovchanskaya, I.V., Ostapenko, A.A., and Fedorenko, Y.V., Wavelet Analysis of High\_Latitude Electric and Magnetic Fluctuations Observed by the Dynamic Explorer 2 Satellite, *J. Geophys. Res.*, 113, A03308 (2008).
24. Jahn, J.M and LaBelle J., Rocket measurements of high-altitude spread F irregularities at the magnetic dip equator *J. Geophys. Res.*, 103, 23,427 (1998).
25. Laundal, K. M., and Gjerloev J. W., What is the appropriate coordinate system for magnetometer data when analyzing ionospheric currents?, *J. Geophys. Res. Space Physics*, 119, 8637–8647, doi:10.1002/2014JA020484 (2014).
26. Le, G., Huang, C.S., Pfaff, R.F., Su, S.Y., Yeh, H.C., Heelis, R.A., Rich, F.J. and Hairston, M., Plasma density enhancements associated with equatorial spread F: ROCSAT-1 and DMSP observations, *Journal of Geophysical Research: Space Physics*, 108, (2003).
27. Molchanov, O. et al., Lithosphere-atmosphere-ionosphere coupling as governing mechanism for preseismic short-term events in atmosphere and ionosphere, *Natural Hazards and Earth Syst. Sci.* 4, 757-767 (2004).
28. Molchanov, O.A., Akentieva, O.S., Afonin, V.V., Mareev, E.A. and Fedorov, E., Plasma density-electric field turbulence in the low-latitude ionosphere from the observation on satellites; possible connection with seismicity. *Physics and Chemistry of the Earth, Parts A/B/C*, 29(4-9), pp.569-577 (2004).
29. Onwumechili, C. A., *The Equatorial Electrojet*, Gordon and Breach Science Publishers, Amsterdam, The Netherlands (1997).
30. Ossakow, S. L. and Chaturvedi, P. K., Current Convective Instability in the Diffuse
31. Aurora, *Geophys. Res. Letters* 6, 332 (1979).

32. Parkinson, M. L., Dynamical critical scaling of electric field fluctuations in the greater cusp and magnetotail implied by HF radar observations of F-region Doppler velocity, *Ann. Geophys.*, 24, 689–705 (2006).
33. Richmond, A. D., Matsushita, S., and Tarpley, J. D.: On the production mechanism of electric currents and fields in the ionosphere, *J. Geophys. Res.*, 81, 547 (1976).
34. Richmond, A. D., Ionospheric electrodynamics using magnetic apex coordinates, *J. Geomag. Geoelectr.*, 47, 191 – 212 (1995).
35. Taylor, G. I., The spectrum of turbulence. *Proc. R. Soc. London*, 164 (919), 476, (1938).
36. Tam, S., Chang, W.Y., Kintner, P.M., and Klatt, E., Intermittency Analyses on the SIERRA Measurements of the Electric Field Fluctuations in the Auroral Zone, *Geophys. Res. Lett.*, 32, L05109, (2005).
37. Uritsky, V. M., and Pudovkin M. I., Low frequency 1/f fluctuations of the AE-index as a possible manifestation of self-organized-criticality in the magnetosphere, *Annales Geophysicae*, 16, 1580 (1998).
38. Weimer, D.R., Goertz, C.K., and Gurnett, D.A., Auroral Zone Electric Fields from DE 1 and 2 at Magnetic Conjunctions, *J. Geophys. Res.*, 90A, 7479, (1985).
39. Wernik, A. W. and Yeh, K. C.: Chaotic behavior of ionospheric scintillation-modeling and observations, *Radio Sci.*, 29, 135–139, (1994).